^{31}P MAS NMR Study of the Ferrielectric−Paraelectric Transition in Layered $CuInP_2S_6$

X. Bourdon,[†] A.-R. Grimmer,[‡] and V. B. Cajipe*,[†]

Institut des Matériaux Jean Rouxel, 2, rue de la Houssinière, B.P. 32229, 44322 Nantes Cedex 3, France, and Humboldt-Universität zu Berlin, Rudower Chaussee 5, Haus 4.1, D-12484 Berlin, Germany

Received December 8, 1998. Revised Manuscript Received June 10, 1999

The order−disorder ferrielectric−paraelectric transition in lamellar $CuInP_2S_6$ is studied using ^{31}P solid-state MAS NMR spectroscopy. Spectra from a powder sample were recorded at various temperatures between 255 and 355 K with a probe precalibrated for heating or cooling due to magic angle spinning. Two center bands are observed at the lowest measured temperature while only one is detected at the highest temperature. The former two represent the inequivalent positions for the P atoms of the P_2S_6 group which reflect the antiparallel displacements of the polar Cu^{I} and In^{III} sublattices in the ferrielectric phase. The latter corresponds to the appearance of a 2-fold axis through the P−P bond as the Cu^{I} ions undergo double-well hopping motions, and the In^{III} ions occupy on-center sites in the paraelectric phase. At intermediate temperatures, both ferrielectric and paraelectric type resonances contribute to the spectrum at ratios which are *T*-dependent, indicating a transition temperature $T_c = 312 \pm 1$ K (310 ± 1 K) for a warming (cooling) cycle. The chemical shifts of the center bands characteristic of the ferrielectric phase are asymmetrically disposed with respect to that of the paraelectric type signal and exhibit distinct thermal variations; the line widths likewise evolve differently with temperature. Line-narrowing attributable to thermally enhanced motions is observed for the paraelectric type resonance upon warming across the transition. The temperature range for the coexistence of the center bands representative of the two phases is unusually wide (≈70 K), lying mostly below T_c. The presence of the ferrielectric type resonance in the paraelectric regime may be ascribed to the nucleation of polar order, while the persistence of the paraelectric signal well below T_c implies residual hopping motions occurring in the ferrielectric regime.

Introduction

The defining characteristic of a ferroelectric system is the existence of a reversible spontaneous electric polarization. This property is determined by the crystal symmetry and is macroscopic. Apart from bulk level changes that occur during a ferroelectric−paraelectric transition, modifications in the local environment of constituent atoms may be monitored to characterize the loss of polarity. Diffraction measurements yield such information but may be insufficient in detecting very small displacements and distinguishing between static and dynamic positional disorder. Resonance techniques provide the required sensitivity to internal field changes as well as a different time scale. A case in point is the order−disorder transition which occurs below 315(5) K in lamellar $CuInP_2S_6$.[1−5] Solid-state NMR spectroscopy is a particularly suitable method for studying the structural subtleties and dynamics of this phase transformation because of the presence of the nuclei ^{31}P, ^{63}Cu, and ^{115}In in this material.

Electric dipole ordering in $CuInP_2S_6$ has been shown to be *ferri*electric, i.e., the spontaneous polarization $P_s \approx 3\ \mu C\ cm^{-2}$, which appears along the normal to the layer, is generated mainly by polar Cu^{I} and In^{III} sublattices shifted in antiparallel directions relative to the midplane.[2] Figure 1a displays a representation of the $CuInP_2S_6$ ferrielectric structure (monoclinic space group *Cc*): the metal cations and P−P pairs occupy octahedral cages defined by the framework formed by the S atoms. The off-centering of the metal cations is attributable to a second-order Jahn−Teller instability associated with the d^{10} electronic configuration.[6] The antiparallel displacements, 1.6 Å upward for Cu^{I} and 0.2 Å downward for In^{III}, are presumably imposed by energy minimization conditions consistent with long-range electric dipole ordering in a lamellar matrix. A weak downward shift for the P−P pair (of the order of 0.01 Å) has also been observed below 315 K as the ethane-like P_2S_6 groups deform to accommodate the Cu^{I} and In^{III} off-centering.

According to single-crystal X-ray diffraction results,[2] the copper sublattice becomes completely polar only well

[†] Institut des Matériaux Jean Rouxel.
[‡] Humboldt-Universität zu Berlin.

(1) (a) Simon, A.; Ravez, J.; Maisonneuve, V.; Payen, C.; Cajipe, V. B. *Chem. Mater.* **1994**, *6*, 1575. (b) Maisonneuve, V.; Evain, M.; Payen, C.; Cajipe, V. B.; Molinié, P. *J. Alloys and Compounds* **1995**, *218*, 157.
(2) Maisonneuve, V.; Cajipe, V. B.; Simon, A.; von der Muhll, R.; Ravez, J. *Phys. Rev. B* **1997**, *56*, 10860.
(3) Vysochanskii, Yu. M.; Stephanovich, V. A.; Molnar, A. A.; Cajipe, V. B.; Bourdon, X. *Phys. Rev. B* **1998**, *58*, 9119.
(4) Cajipe, V. B.; Payen, C.; Bourdon, X.; Mutka, H.; Schober, H.; Frick, B. *ILL Exp. Report 4-02-295* **1996**.
(5) Vysochanskii, Yu. M.; Molnar, A. A.; Stephanovich, V. A.; Cajipe, V. B.; Bourdon, X. *Ferroelectrics* **1999**, in press.

10.1021/cm980776n CCC: $18.00
Published on Web 10/01/1999

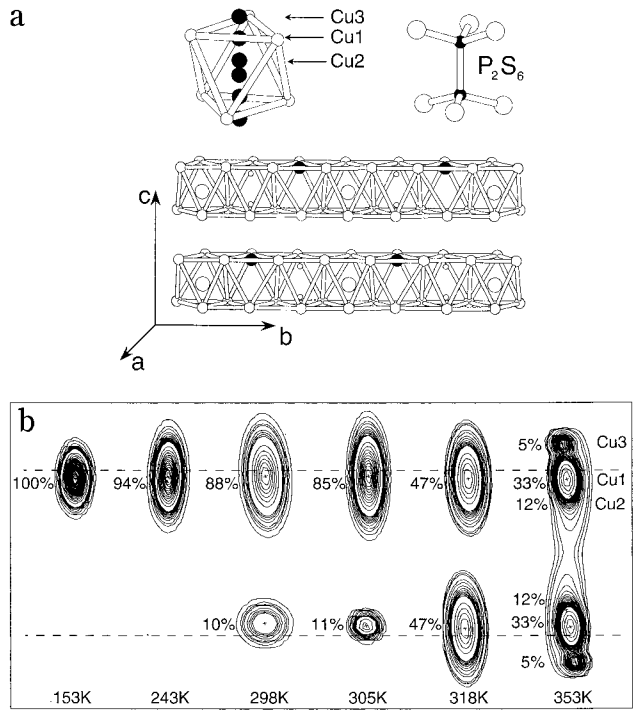

Figure 1. (a) Top left: Sulfur octahedral cage showing the various types of copper sites, including the off-center Cu1, the almost central Cu2 and the Cu3 in the interlayer space. Two off-center sites become inequivalent when unequally occupied. Top right: The ethane-like P_2S_6 group. Bottom: Perspective view of two layers of $CuInP_2S_6$ shown in the ferrielectric phase (space group *Cc*, $T < 315$). The framework is formed by the S atoms. The up (down) shifted Cu^I (In^{III}) ions are represented by the larger black (white) circles in the octahedra; the smaller white circles are the P atoms. A projection onto the plane of a layer would reveal triangular arrays of Cu^I, In^{III}, and $(P_2S_6)^{-4}$ ions (not shown; see ref 2). The monoclinic cell parameters at room temperature are $a = 6.0956(4)$ Å, $b = 10.5645$ Å, $c = 13.6230(9)$ Å and $\beta = 107.101(3)°$. (b) Thermal evolution of the different copper site occupancies and the corresponding probability density contours in $CuInP_2S_6$ (see ref 2). Sites Cu1, Cu2, and Cu3 are disposed along the layer normal. The crosses mark the refined positions, and the dashed lines indicate the upper and lower sulfur planes of a single layer. Occupancies not adding up to 100% indicate the presence of diffuse electronic densities between the off-center sites and/or in the interlayer space. The contours are given in $Å^{-3}$, the values for the lowest and highest displayed temperatures being as follows: 153 K, 25−75 (50), 75−775 (100) and 775−27775 (1000); 353 K, 40−100 (30), 100−800 (100) and 800−5800 (1000), where the intervals are given in parentheses.

below the transition. Indeed, evidence has been found at $240 < T < 315$ K for copper occupation of a lower off-center site, or diffuse electronic densities thereabout, as well as residual densities around the central region. Figure 1b reproduces a picture from ref 2, which summarizes the thermal variation of the copper site occupancies and the corresponding probability density contours in the 153−353 K range. In the paraelectric phase (space group *C*2/*c*), the crystallographic model requires the use of three types of partially filled copper sites with large thermal factors: an off-center and quasi-trigonal Cu1, an almost central or octahedral Cu2, and a third nearly tetrahedral Cu3 in the interlayer space. The Cu^I probability density then assumes a shape that is 2-fold symmetric about the center of the octahedral CuS_6 group and extends along the layer normal and into the interlamellar space. Simultaneously, the In^{III} position and midpoint of the P−P bond move into the layer midplane. The contour plots for the copper probability density exhibit maxima only around Cu1 and Cu3 type sites. This is consistent with a dynamic interpretation of the disorder which has been corroborated by Raman spectroscopy[3], inelastic neutron scattering,[4] and dielectric measurement[5] data. In other words, at $T > 315$ K, the Cu^I ions hop between the minima of a double-well potential (Cu1) and between one such minimum and an interlayer site (Cu3). The occupation of site Cu2 thus merely represents the probability of finding the Cu^I in the central region as these motions occur. Ordering takes place via a cooperative freezing of the inter-site hopping which breaks the 2-fold symmetry and locks in a net polarization. Displacive transitional behavior associated with the In^{III} has not been evidenced.[3] This order−disorder phase transition has been shown to be first order.[1−3,5] At $T \gg T_c$, ion migration through the lattice has also been detected.[5,7]

In this paper, we present a ^{31}P solid-state MAS NMR spectroscopy study of $CuInP_2S_6$. While the ^{31}P nuclei do not play a key role in the phase transition, they are good indicators of the symmetry-breaking process because the 2-fold axis of the paraelectric structure runs through the midpoints of the P−P pairs. Specifically, a pronounced inequivalence of the upper and lower nuclei of a pair is expected as a consequence of antiparallel distortions caused by opposite Cu^I and In^{III} displacements. Our approach here is to follow the thermal evolution of the relative contributions, chemical shifts and line widths of the resonances in the phosphorus NMR spectrum. To guarantee correct temperature readings, the probe was precalibrated for sample heating or cooling due to magic angle spinning.[8] A qualitative discussion of the dynamics in this system is also given based on the spectral features and preliminary measurements of the spin−lattice relaxation time.

Experimental Section

$CuInP_2S_6$ was synthesized by high temperature reaction of the elements in an evacuated tube as previously described.[1,2] The product was ground to prepare the powder samples; grain sizes were in the ≤50 μm range. ^{31}P MAS NMR spectra were recorded on a MSL 400 spectrometer operating at $\nu_0 = 161.9$ MHz and using a standard Bruker MAS probe with a double-bearing rotation system. The spinning rate was stabilized to ±3 Hz using a Bruker pneumatic unit. Samples were loaded into zirconia rotors 4 mm in diameter and with KelF caps. Preliminary ^{31}P MAS NMR measurements on $CuInP_2S_6$ at room temperature revealed a significant and reversible de-

(6) (a) Burdett, J. K. *Chemical Bonding in Solids*; Oxford University Press: Oxford, England, 1995; p 24 and p 246. (b) Burdett, J. K.; Eisenstein, O. *Inorg. Chem.* **1992**, *31*, 1758. (c) Wei, S. H.; Zhang, S. B.; Zunger, A. *Phys. Rev. Lett.* **1993**, *70*, 1639. (d) The distortion of the octahedral environment of a d^{10} cation in a lamellar hexathiohypodiphosphate was first attributed to a second-order Jahn−Teller effect by: Lee, S.; Colombet P.; Ouvrard G.; Brec, R. *Inorg. Chem.* **1988**, *27*, 1291. (e) The mentioned distortion for Cd^{II} in $Cd_2P_2S_6$ was studied by means of LMTO−ASA and extended Hückel methods in: Zhukov, V.; Boucher, F.; Alemany, P.; Evain, M.; Alvarez, S. *Inorg. Chem.* **1995**, *34*, 1159. We have carried out similar LMTO calculations for $CuInP_2S_6$ and confirmed that the Cu^I off-centering normal to the layer is consistent with a hybridzation of the 3d and 4s bands.

(7) Maisonneuve, V.; Réau, J. M.; Dong, M.; Cajipe, V. B.; Payen, C.; Ravez, J. *Ferroelectrics* **1997**, *196*, 257.

(8) Grimmer, A. R.; Kretschmer, A.; Cajipe, V. B. *Magn. Reson. Chem.* **1997**, *35*, 86.

pendence of the spectral features on the spinning rate: two resonances at 3−5 kHz, one at 15 kHz, and a combination of all three at intermediate rates. This observation was attributed to frictional sample heating. To quantify this effect, an empirical expression for the sample temperature T_s was determined in a separate set of experiments using $Sm_2Sn_2O_7$ as a chemical shift thermometer:

$$T_s = 0.12\nu_r^2 + (3.47-0.013T_b)\nu_r + 0.80T_b + 58.6 \quad (1)$$

where T_b (K) is the bearing gas temperature and ν_r (kHz) is the spinning rate.[8] For example, spinning to 16 kHz raises the nominal room temperature to 321 K. Spectra were subsequently recorded upon warming between $T_b = 223$ and 353 K ($T_s = 254.7$ and 341.8 K) at a MAS rate of 10 kHz to obtain maximal resolution and eliminate magnetic dipolar and chemical shift anisotropy effects. Measurements were also made in a cooling cycle with $298 < T_b < 353$ K. Difficulties associated with maintaining a high spinning rate while cooling precluded extending the measurements to lower temperatures. The limited cooling range however covers the temperatures of interest. As in the temperature calibration experiments, the bearing gas was cooled or heated while the driving gas was maintained at ambient temperature. The bearing gas pressure was adjusted to 3 bar and the temperature controlled by the Bruker VT unit using the probe head thermocouple. ^{31}P chemical shifts were referenced to the signal for H_3PO_4 and measured to a precision of ±0.06 ppm. The room temperature was stabilized to ±0.2 K to suppress measurable fluctuations in the chemical shift. After each temperature change, the sample was allowed to equilibrate for 10 min before starting the next measurement. Under these thermal conditions, no temperature gradients greater than 1 K should exist within the rotor.[8] Other typical parameters used in the single pulse experiments were: a 90° pulse length of 2 μs, a 60 s relaxation delay, a number of scans equal to 8 and a spectrum width of 32.5 kHz. T_1 measurements were performed under static conditions using the same spectrometer and an inversion−recovery pulse sequence $\pi-\pi-\pi/2$.

Data analysis was carried out using the commercial programs WINNMR and WINFIT. Deconvolution employed line shapes of mixed Gaussian−Lorentzian character.

Results and Discussion

An overview of our variable temperature ^{31}P NMR results is given by the center bands shown in Figure 2, recorded during a warming cycle. These central features contain the essential information, since less than 5% of the integrated intensity of each complete spectrum is accounted for by the sidebands; also, the chemical shift anisotropy and magnetic dipole coupling were noted to be identical for the various resonances observed. The temperature indicated for each spectrum in Figure 2 was evaluated from the bearing gas temperature using eq 1 with a spinning rate $\nu_r = 10$ kHz. The thermal evolution of the resonances found here agrees with the observation of spectral changes induced by increasing the spinning rate at constant bearing gas temperature (see previous section). At temperatures far below the transition, the spectrum exhibits two center bands with an approximate 1:1 intensity ratio; well above T_c, only one band appears. Identification of these peaks is straightforward. The two lines observed at $T_b = 223$ K ($T_s = 254.7$ K) correspond to the two inequivalent positions for phosphorus in the ferrielectric phase; the lower and higher frequency signals shall here be referred to as the A and B resonances, respectively. The one line at $T_b = 353$ K ($T_s = 341.8$ K), designated C, corresponds to the single crystallographic *P* site of the paraelectric phase. Within a fairly wide thermal range enclosing T_c, both the low and high-temperature type resonances contribute to the spectrum at ratios that are *T* dependent. Very similar thermal variations were found in the data recorded in a cooling cycle.

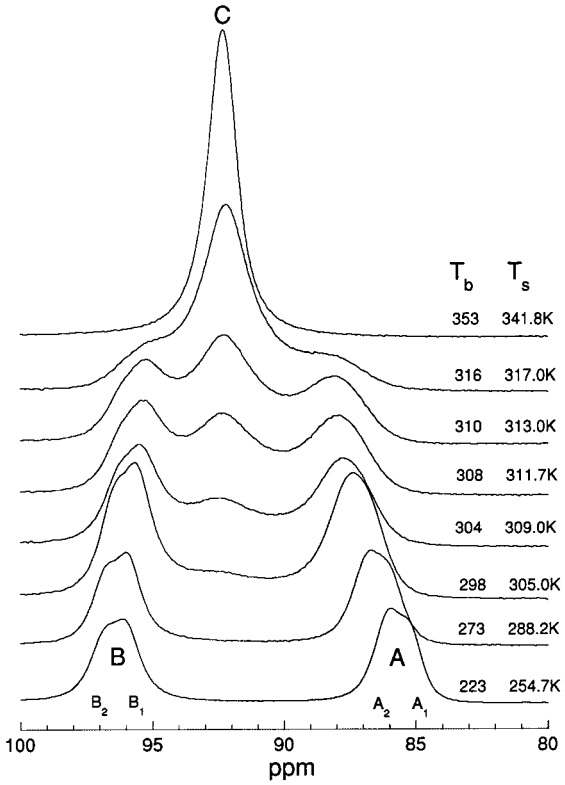

Figure 2. ^{31}P MAS NMR spectra recorded from $CuInP_2S_6$ at bearing temperature $T_b = 223$, 273, 298, 304, 308, 310, 316, and 353 K. The corresponding sample temperatures T_s are also indicated.

The observation of only one line at the highest temperature is consistent with a dynamic character for the copper disorder in the paraelectric phase. Given that the Cu^I ions occupy sites that are off the layer midplane at all temperatures, the single line implies that the P nuclei within a P_2S_6 group become indistinguishable because the neighboring copper ions undergo rapid motions within a 2-fold-symmetric potential. These copper motions may be said to result in an effective exchange process between the paired ^{31}P nuclei which occurs at a rate determined by the separation in Hz of the two signals A and B, here estimated to be about 3846 Hz at $T_s = 254.7$ K for the observing frequency ν_0.[9a,10] The chemical shift of the line at high temperature (92.37 ppm at $T_s = 341.8$ K) does not coincide with the mean position of the two signals observed at low temperature (91.08 ppm at $T_s = 254.7$ K). This signifies that the phosphorus environment in the paraelectric phase is not a simple motional average of that for $T < T_c$. Such an observation is consistent with the off-centering of the P−P centroid in the ferrielectric phase.[2] The superposition of signals characteristic of the ferri- and paraelectric phases at intermediate temperatures

(9) Friebolin, H. *Basic One- and Two-Dimensional NMR Spectroscopy*; VCH Publishers: New York, 1991: (a) p 269, where the rate constant is given by 2.22 $\Delta\nu$; (b) p 102.

(10) Abragam, A. *Principles of Nuclear Magnetism*; Oxford University Press: Oxford, England, 1961; p 425.

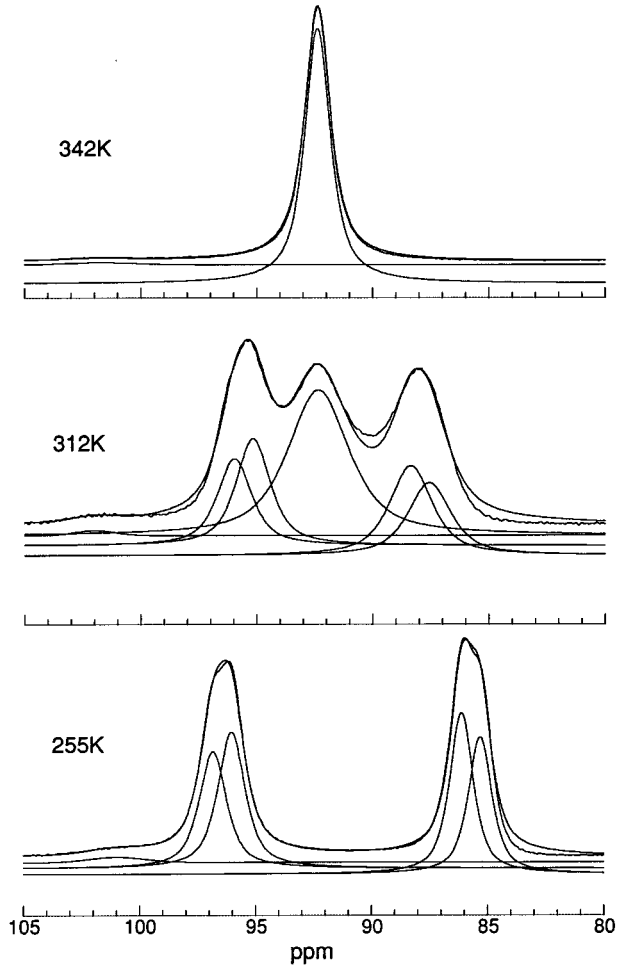

Figure 3. Deconvolution of ^{31}P MAS NMR spectra using mixed Gaussian−Lorentzian line shapes at representative temperatures T_s.

agrees with the transition being first-order, i.e., the occurrence of phase coexistence.

A more quantitative description of the above findings may be obtained by performing an iterative deconvolution analysis of the complete data set. Figure 3 displays the decomposition into Gaussian−Lorentzian peaks for a representative subset of spectra. The small *T*-independent signal at 101.7 ppm is attributable to Cu_3PS_4, an impurity which often forms during the synthesis of $CuInP_2S_6$; its contribution was taken into account during the analysis and evaluated at 1.5%. The deconvolution was complicated by the temperature dependence of the chemical shifts as well as the asymmetry of the resonances characteristic of the ferrielectric phase. The intensity distribution of the low-*T* spectrum exhibits the "roof effect" typical of a second-order spectrum, specifically that of an AB spin system[9b] rarely observed in solid-state materials.[11] Application of resolution enhancement techniques reveals a clear splitting of the two signals into A_1-A_2 and B_1-B_2 doublets as shown in Figure 4 for $T_s = 254.7$ K. Careful adjustment of the spectral line shape parameters yielded a P−P coupling constant $J = 130$ Hz. The value of J was assumed to be constant within the investigated temperature region; the known weak *T* dependence of the

(11) Eichele, K.; Wu, G.; Wasylishen, R. E.; Britten, J. F. *J. Phys. Chem.* **1995**, *99*, 1030.

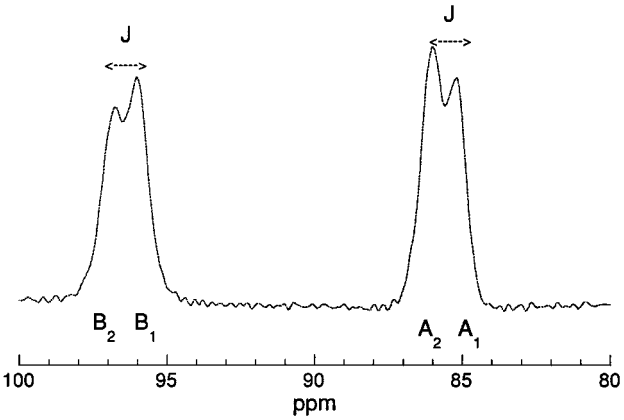

Figure 4. ^{31}P MAS NMR spectrum obtained at $T_s = 254.7$ K using resolution enhancement techniques to reveal splitting due to P−P coupling.

P−P bond length[2] and the quality of the fits thus obtained prove this is a reasonable assumption. For a given *T*, the same line width for the components of a doublet was used. On the other hand, the widths of the two doublets were found to be very different. Equal intensity contributions were assumed for resonances A and B. The relative intensities within a doublet were constrained as normally expected for an AB system such that

$$I_{A1}/I_{A2} = I_{B1}/I_{B2} = (1 + \sin 2\theta)/(1 - \sin 2\theta)$$

where $\sin 2\theta = J[(\nu_0\delta)^2 + J^2]^{1/2}$, and $\delta = |(\delta_{A1} + \delta_{A2})/2| - |(\delta_{B1} + \delta_{B2})/2)|$, the subscripted δ's being the chemical shifts determined for each peak. As T_c is approached from below, the doublets are no longer resolved. In the paraelectric regime, the single band C is representative of an A2 type system.

On the basis of the intensities calculated in the deconvolution, the percentage contributions of the A + B and C resonances to the total spectrum may be plotted vs temperature as displayed in Figure 5. The derivative of the percentage C contribution with respect to *T* attains a maximum at 312 ± 1 K (310 ± 1 K) for the warming (cooling) curve. This agrees well with the T_c and thermal hysteresis determined by dielectric measurements and calorimetry (315 ± 5 K).[1] The shape of the more complete A + B curve of the warming cycle also closely matches that of the spontaneous polarization $P_s(T)$ calculated from crystallographic results.[2] Importantly, Figure 5 shows that the C resonance is detectible down to $T_s = 261.4$ K and the A + B bands up to 328.4 K. This is a remarkably wide temperature range for "phase coexistence", which merits further discussion (see below).

More detailed information is uncovered by plotting the chemical shifts of the various resonances as a function of temperature (Figure 6). The asymmetric disposition of the A and B resonances with respect to C is made very clear here. All three curves exhibit an inflection point around 312 K (310 K) for the warming (cooling) cycle, as confirmed by evaluating the derivatives. An appreciable *T* dependence is observed for the chemical shift of A even below T_c, while that for B appears to be constant at $254.7 < T_s < 288.2$ K. A reasonable interpretation of these results may be given by assigning resonance A (B) to the lower (upper)

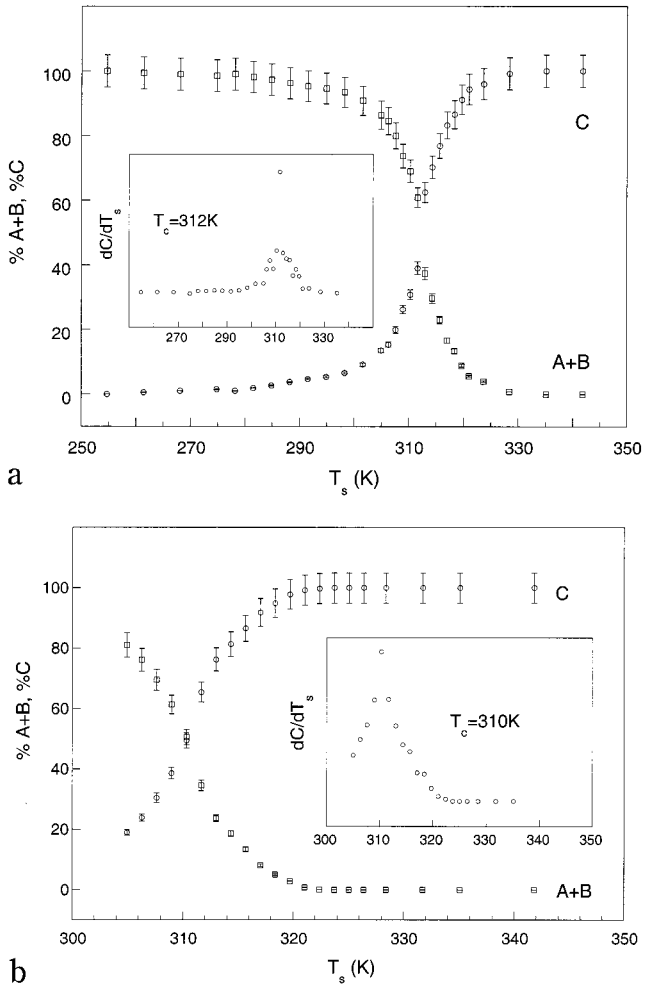

Figure 5. Percentage contributions of the A + B and C resonances to the total spectrum calculated from the respective integrated intensities as a function of temperature for the (a) warming and (b) cooling cycles. The insets show the derivative of the percent C contribution and indicate the T_c deduced from the maximum.

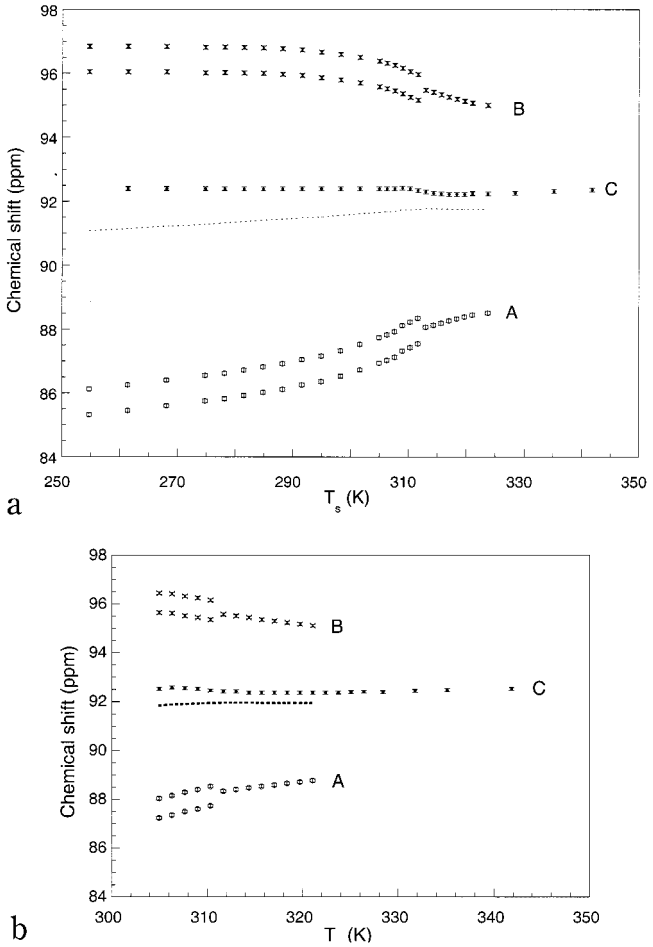

Figure 6. Thermal evolution of the chemical shifts for the various resonances upon (a) warming and (b) cooling. The positions of the A and B doublet components are given when resolved ($T < T_c$); the mean positions of A and B as a function of T are indicated by the dashed curve.

phosphorus of the pair. P_B would be in the vicinity of the upshifted Cu^I (upper Cu1 site), while P_A would be close to the downshifted In^{III} and the lower Cu1 site which may have a nonzero occupancy below T_c. According to the known ferrielectric structure, the P_B-S bonds are longer than the P_A-S. This is consistent with the assumed assignment since the shielding for P_A may then be said to be stronger than for P_B, so that the P_A resonance frequency is lower. Crystallographic results have also shown that the In^{III} displacement increases while the occupation of the lower Cu1 site decreases with cooling below T_c. Figure 6 implies that thermal modifications in the surroundings of P_A accompanying such changes are more pronounced than those generated around P_B as the upper Cu1 site occupancy approaches 100%. While geometric differences between the upper and lower PS_3 pyramids are clearly evidenced by X-ray diffraction in the ferrielectric regime, the temperature behavior of the bond lengths and angles of each PS_3 group is rather subtle and barely detected using this technique.[2,3] The curves of Figure 6 thus illustrate the greater sensitivity of NMR to such fine, local changes (lengths <0.001 Å; angles <0.5°).[12]

As mentioned earlier, the A and B resonances also differ in their line widths. The A_1-A_2 doublet is narrower than the B_1-B_2 doublet at the lowest measured temperature (194 vs 227 Hz at 255 K). Both broaden as T increases, the former at a faster rate so that it is wider than the latter at T_c (356 vs 291 Hz). This is visible in the temperature dependence of the relative peak amplitudes (Figures 2 and 3), following the conservation of the 1:1 intensity ratio for A and B. The difference in width may be due to distinct coupling effects between each type of P nucleus and a neighboring quadrupolar nuclear moment. Coupling between phosphorus and spin $^9/_2$ indium and spin $^3/_2$ copper nuclei is likely given the natural abundances of ^{115}In (95.7%), ^{63}Cu (69.1%), and ^{65}Cu (30.9%), and their relative receptivities (3.38×10^{-1}, 6.45×10^{-2}, and 3.55×10^{-2}, respectively[13]). ^{31}P NMR broadening due to coupling with the indium nucleus has in fact been observed in static spectra of $In_{4/3}P_2S_6$[14] and should be present in $CuInP_2S_6$ as well. The peak broadening occurs as the A and B chemical shifts approach that of C, thus leading to the nonresolution of the doublets at higher temperatures. These effects may be related with the growing percent-

(12) Grimmer, A. R. *Mol. Phys.* **1987**, *60*, 151.

(13) Harris, R. K. *Nuclear Magnetic Resonance Spectroscopy*; John Wiley and Sons: New York, 1986; p 238.

(14) Bourdon, X.; Grimmer, A. R.; Cajipe, V. B. Unpublished results.

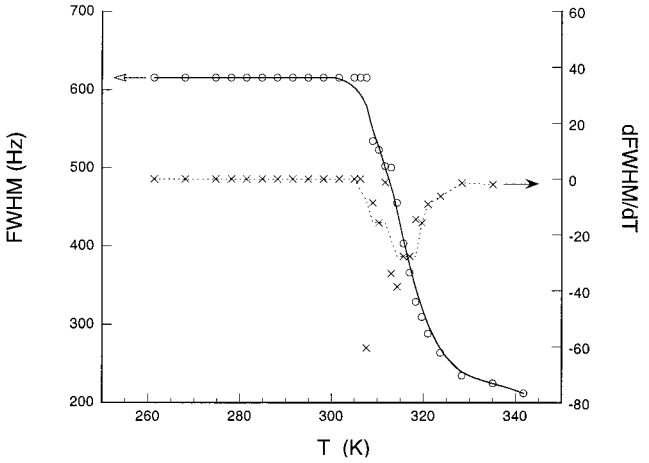

Figure 7. Line width of resonance C plotted vs temperature and its derivative.

age of signal C measured between 290 K and T_c (Figure 5).

The simultaneous presence of A + B and C resonances within a wide temperature range is also made plain by Figure 6. Given the inflection in all of the curves around 312 K, it may be said that the environment for each type of resonating nucleus in the paraelectric regime is distinct from that in the ferrielectric regime. The T dependence of the chemical shifts for A and B is much weaker and more similar for the two branches above T_c than below. The difference between the T-behavior of the chemical shift for C in the two regimes is less clear. On the other hand, the line width of resonance C, which was satisfactorily modeled by a large, constant value (615 Hz) for $T < T_c$ is observed to decrease when warming above T_c (Figure 7). The Gaussian-to-Lorentzian character ratio of the line shape also decreases at $T > T_c$ (e.g., 0.3 at 261 K and 0.0 at 324 K). This line-narrowing may be attributed to thermally enhanced motions. Figure 7 suggests that the attainment of full narrowing requires heating above 342 K. Ionic conductivity is known to occur in this higher temperature range.[5,7] Copper migration through the lattice is complex, involving double-well motions, passage through the basal triangles of the S_6 octahedral cage, and hopping within the interlayer space. The width of the C resonance width may be said to to reflect an effective copper hopping frequency: interpreted within a cooling cycle, its T dependence in the paraelectric regime may be related to the slowing down of these 2-fold symmetric motions which then triggers the first-order transition. Indeed, the derivative of the line width with respect to temperature drops within a 10 K interval around T_c (Figure 7). The detailed features of the derivative curve in the said interval might be associated with the presence of motions other than intra-cage, double-well hopping; on the other hand, these may be due to the less accurate modeling of the width at $T < T_c$. Copper motions that remain active below T_c thus conceivably occur at frequencies lower than in the paraelectric phase.

The 70 K wide temperature range for the coexistence of the A + B and C resonances lies mostly within the ferrielectric regime. In a cooling cycle, the presence of A + B in the paraelectric regime may be ascribed to nucleation, i.e., the appearance of small polar regions

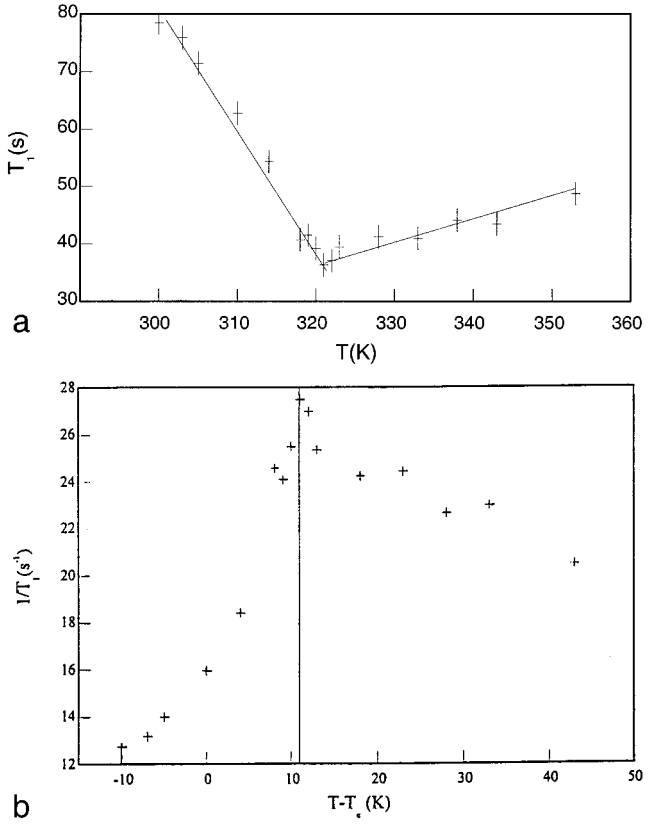

Figure 8. (a) The T dependence of T_1, obtained in a cooling cycle between 353 and 300 K. (b) T_1^{-1} vs $T - T_c$.

within a crystallite as the copper hopping motions slow and become correlated. This implies the existence of some kind of short-range order at $T > T_c$ that has yet to be detected using diffraction methods. The persistence of C at 260 K implies that copper hopping motions occur down to that temperature. Long-range polar order in $CuInP_2S_6$ may then be envisioned as nucleating in the central areas of the innermost layers and extending to the crystallite surfaces with cooling. Upon reaching T_c, 2-fold symmetry is broken in the bulk but residual motions remain in the peripheral regions. In a warming cycle, loss of order would correspond to reversing this scenario. The minority occupation of the lower Cu1 site within the ferrielectric regime evidenced by diffraction (Figure 1b) was previously interpreted in terms of occasional motions of the upshifted copper ion into a shallower, downshifted potential minimum or of reversely polar domains in the crystal[2]. The present NMR data indicate that this observation may also be accounted for by residual copper hopping in the superficial, nonpolar regions of a crystal. Such an effect may be expected to become less visible with increasing grain size; i.e., the contribution of resonance C to the spectral intensity at $T < T_c$ would be smaller for a large single crystal than for a fine powder sample.

Measurements of the spin−lattice relaxation time T_1 were undertaken originally as a precaution against saturation effects. Some information on the local dynamics characteristic of the paraelectric and ferrielectric regimes can however be extracted by plotting out the T dependence of the results. Figure 8a shows that the relaxation time vs temperature curve, obtained in a cooling cycle between 353 and 300 K, exhibits a minimum at 322 K. Alternatively, plotting T_1^{-1} vs $T - T_c$

shows that the relaxation rate increases moderately between 353 and 322 K and then drops rapidly thereafter (Figure 8b). An analogy might be drawn between the latter finding and those for other order−disorder ferroelectrics, e.g., KD_2PO_4 or dicalcium strontium propionate, in which the deuteron or proton relaxation rate diverges at the transition.[15] On the other hand, the maximum relaxation rate here is observed at a temperature higher than T_c; this result was confirmed in three sets of experiments. It may be argued that the intrinsic dynamics of the symmetry-breaking process in $CuInP_2S_6$ is masked by the coexistence of polar and nonpolar regions within a crystallite at temperatures close to T_c. Moreover, the probability of finding copper in an interlayer site is known to be nonzero in the ferrielectric regime.[2] No changes in slope were however evident in the plots of magnetization vs τ (time interval between saturating and read pulses) used to determine T_1 in $CuInP_2S_6$, i.e., only one relaxation time could be detected at each temperature. The peak in the relaxation rate at $T = 322$ K (Figure 8b) happens to coincide with the highest temperature at which the resonances A and B appear in the paraelectric regime. It may conceivably also be associated with the deactivation of ionic conductivity. These initial observations indicate the importance of performing more detailed experiments to sort out the various types of copper hopping motions and fully describe the transitional relaxation dynamics in $CuInP_2S_6$. In particular, T_1 and T_2 measurements should be made at different operating frequencies and using finer temperature increments for both ^{31}P and ^{63}Cu nuclei. The contributions of chemical shift anisotropy, dipole−dipole and electric quadrupolar mechanisms to the relaxation may likewise be thus determined. These experiments shall be carried out soon.

(15) Lines, M.; E.; Glass, A. M. *Principles and Applications of Ferroelectrics and Related Materials*; Clarendon Press: Oxford, England, 1979; pp 417−422. Although the resonating nuclei in the present study are not responsible for the critical dynamics in $CuInP_2S_6$, the analogy is valid to the extent that the ^{31}P environment is sensitive to the copper hopping motions.

Acknowledgment. We are grateful to A. Kretschmer for technical assistance. V.B.C. and X.B. acknowledge helpful discussions with C. Payen and partial support from the European Commission via Contract No. IC15-CT97-0712.

CM980776N